HHS Public Access

Author manuscript

Cancer Res. Author manuscript; available in PMC 2017 June 01.

Published in final edited form as:

Cancer Res. 2016 June 1; 76(11): 3156–3165. doi:10.1158/0008-5472.CAN-15-2528.

Myeloid-derived suppressor cells endow stem-like qualities to breast cancer cells through IL-6/STAT3 and NO/NOTCH cross-talk signaling

Dongjun Peng[1], **Takashi Tanikawa**[1], **Wei Li**[1], **Lili Zhao**[2], **Linda Vatan**[1], **Wojciech Szeliga**[1], **Shanshan Wan**[1], **Shuang Wei**[1], **Yin Wang**[1], **Yan Liu**[1], **Elzbieta Staroslawska**[3], **Franciszek Szubstarski**[3], **Jacek Rolinski**[4], **Ewelina Grywalska**[4], **Andrzej Stanisławek**[5], **Wojciech Polkowski**[6], **Andrzej Kurylcio**[6], **Celina Kleer**[7,8], **Alfred E. Chang**[1,8], **Max Wicha**[8,9], **Michael Sabel**[1,8], **Weiping Zou**[1,8,10], and **Ilona Kryczek**[1]

[1]Department of Surgery, University of Michigan School of Medicine, Ann Arbor, MI [2]Department of Biostatistics, University of Michigan School of Medicine, Ann Arbor, MI [3]St. John's Cancer Center, Lublin, Poland [4]Department of Clinical Immunology, Medical University of Lublin, Lublin, Poland [5]Department of Oncology, Medical University of Lublin, Lublin, Poland [6]Department of Surgical Oncology, Medical University of Lublin, Lublin, Poland [7]Department of Pathology, University of Michigan School of Medicine, Ann Arbor, MI [8]University of Michigan Comprehensive Cancer Center, University of Michigan School of Medicine, Ann Arbor, MI [9]Department of Medicine, University of Michigan School of Medicine, Ann Arbor, MI [10]Graduate Programs in Immunology and Tumor Biology, University of Michigan School of Medicine, Ann Arbor, MI

Abstract

Myeloid-derived suppressor cells (MDSC) contribute to immune suppression in cancer, but the mechanisms through which they drive metastatic progression are not fully understood. In this study, we show how MDSC convey stem-like qualities to breast cancer cells that coordinately help enable immune suppression and escape. We found that MDSC promoted tumor formation by enhancing breast cancer cell stem-like properties as well as by suppressing T cell activation. Mechanistic investigations indicated that these effects relied upon crosstalk between the STAT3 and NOTCH pathways in cancer cells, with MDSC inducing IL-6-dependent phosphorylation of STAT3 and activating NOTCH through nitric oxide (NO), leading to prolonged STAT3 activation. In clinical specimens of breast cancer, the presence of MDSC correlated with the presence of cancer stem-like cells (CSC) and independently predicted poor survival outcomes. Collectively, our work revealed an immune-associated mechanism that extrinsically confers cancer cell

Correspondence: Weiping Zou, MD, PhD, University of Michigan School of Medicine, BSRB, 109 Zina Pitcher Place, Ann Arbor MI 48109-0669, ; Email: wzou@umich.edu; Ilona Kryczek, PhD, University of Michigan School of Medicine, BSRB, 109 Zina Pitcher Place, Ann Arbor MI 48109-0669, ; Email: ilonak@umich.edu

Author contributions

I.K. and W.Z. designed the research and wrote the paper. I.K., D.P., T.T., L.V., W.S., W.L., S.W., S.W., Y.W., and Y.L. performed experiments. I.K. and L.Z. analyzed data. E.S., F.S., J.R., E.G., A.S., W.P., A.K., C.K., A.E.C., M.W., and M.S. provided important intellectual and technical support, clinical specimens, and clinical and pathological information. All authors read and approved the manuscript.

Conflict-of-interest disclosure: The authors declare no competing financial interests.

stemness properties and affects patient outcome. We suggest that targeting STAT3-NOTCH crosstalk between MDSC and CSC could offer a unique locus to improve cancer treatment, by coordinately targeting a coupled mechanism that enables cancer stemness and immune escape.

Keywords

Myeloid derived suppressor cell; STAT3; IL-6; NO; T cell immunity; breast cancer; cancer stem cell; NOTCH; survival

Introduction

The capacity of immunity to control and shape cancer progression ([1,2]) has been the subject of intensive investigation. Active protective immunity contributes to tumor dormancy during immunoediting ([3]). Inhibitory immune elements form immune suppressive networks in the tumor microenvironment and are the main obstacles for developing effective cancer immunotherapies ([4,5]). However, it is poorly understood whether the immune suppressive networks reshape cancer and cancer dormancy in specific human cancer, and in turn impact tumor progression, metastasis and therapeutic response in the immune competent host.

It is thought that dormant cancer cells may be stem-like cells with high metastatic and therapeutic resistant potential. The definition of cancer stem cells (CSCs) remains largely operational. Nonetheless, CSCs are thought to be involved in tumor initiation, progression, metastasis and therapy resistance ([6–8]). *In vivo*, the stemness of cancer cells is not exclusively intrinsic to cancer stem cells. Extrinsic mechanisms ([9]) provided by the tumor microenvironment may be essential for forming the stem cell niche ([10]). For example, mesenchymal stem cells ([10]), myeloid cells ([11–13]) and T cell subsets ([14,15]) promote tumor metastasis. It is poorly understood if breast CSCs are the primary targets of these cells ([10,14,16,17]).

STAT3 activation is often observed in cancers, particularly metastatic sites ([18,19]). Persistently activated STAT3 in tumor cells acts as a crucial oncogenic mediator and promotes tumorigenesis ([18,20–23]). Many factors can activate transiently STAT3. However, it is not well understood how STAT3 is persistently activated in the cancer cells and what is the functional and clinical consequence of persistent STAT3 activation in human breast cancer.

In this report we outline extensive studies on the interaction between MDSCs and CSCs in animal models and patients with breast cancer, dissect cellular and molecular mechanisms by which MDSCs reshape breast cancer stemness via STAT3 and NOTCH cross-talk, and reveal the pathological, clinical and therapeutic relevance of the interaction between MDSCs and CSCs in breast cancer.

Materials and Methods

Human subjects, tissues and cells

Patients diagnosed with breast cancer were recruited in the studies. All use of human subjects in this study was approved by the local Institutional Review Boards (IRB). We collected fresh breast cancer tissues from the University of Michigan Surgery Clinic. Fresh tumors were processed into single cell suspension and immediately used for MDSC and tumor (stem) cell analysis ([13,15,24,25]). Specifically, tumor cell suspensions were prepared from solid tumors by enzymatic digestion in 50 mL of HBSS (Life Technologies) containing 40 mg of collagenase, 4 mg of DNase I, and 100 units of hyaluronidase (Sigma Co.) for 2 hours. Cells were washed twice in HBSS. MDSCs were enriched by depleting tumor cells, B and T cell subsets (PE-selection kit, StemCell Technology, Vancouver, Canada) and 7-AAD exclusion, and sorted with high-speed sorter FACSaria (Becton Dickinson, San Jose, CA) to high purity (>97%). We studied formalin-fixed, paraffin-embedded breast cancer tissues from 104 Her-2/neu$^+$ patients in Poland (Cohort 1) ([26,27]), and from 84 breast cancer patients from the University of Michigan School of Medicine (Cohort 2) and 90 breast cancer patients from Poland (Cohort 3) for this study (Supplementary Table 1). Cohort 1 was initially recruited for clinical trials with Herceptin treatment ([26,27]). Cohorts 2 and 3 were randomly recruited regardless of Her-2 expression status. After pathological review, a tissue microarray (TMA) was constructed from the most representative area of paraffin-embedded breast cancer tissues. The TMAs were used for specific immunohistochemistry staining. 593 patients with breast cancer were evaluated in TCGA Breast datasets in Oncomine.org

Immunohistochemistry analysis

Immunohistochemistry staining was performed as previously described ([28–30]). Tissues were stained with polyclonal rabbit anti-human-CD33 (1/10 dilution, DAKO) ([13]), or mouse anti-human ALDH1 (Becton Dickinson) ([24]). We used Horseradish Peroxidase based detection system to detect positive cells (EnVision, DAKO). The specimens were digitalized with an automated platform (Aperio Technologies) and ScanScope XT and Spectrum Plus using TMA software version 9.1 scanning system. Cores were manually scored in high resolution of 40×. A mean score of duplicate cores from each individual tissue was calculated. Any discrepancies were resolved by subsequent consultation with diagnostic pathologist. The cores were quantified and analyzed for the expression of ALDH1 and CD33 with an Aperio imaging system (Genetix). Cytoplasmic expression of ALDH1 was evaluated, whereas nuclear staining alone was considered nonspecific and was not included in the analysis. Intensity of staining was scored as 0 (no expression), 1+ (less than 1% of positive cells), 2+ (1–5% of positive cells), 3+ (5–20% of positive cells), and 4+ (more than 20% positive cells). The intratumoral CD33$^+$ cells were quantified and expressed as the numbers of CD33$^+$ cells per 0.6 mm^2 of tumor section. The tissues were divided into high and low CD33$^+$ cell infiltration based on the median value. The optimal cutoff points were calculated using the R OC curve. HumanVimentin and E-cadherin were detected in paraffin-embedded MCF-7 cells with PathScan® EMT Duplex IF kit (Cell signaling).

Cell lines

MCF-7 and MDA-MB-231 cell lines (ATCC, Manassas, VA) were characterized and authenticated by the vendor using short tandem repeat (STR) DNA profiling. The cell lines were passaged in our laboratory for fewer than 6 months. All cell lines were maintained in DMEM supplemented with 10% FBS plus 100 U/ml penicillin and 100 μg/ml streptomycin (P/S).

Human xenograft tumor model

Human xenograft tumor model was established in female NOD-scid IL2Rγnull (NSG) mice with modifications ([13,24,25]). Briefly, MCF-7 breast cancer cells plus MDSCs were mixed with anti-IL-6 (200 μg, mouse IgG2b, R&D) and iNOS inhibitor (L-NMMA, 50 μmol, EMD Millipore), and were subsequently inoculated subcutaneously into NSG mice supplied with estradiol-17β pellet. Tumor development was monitored and tumor size was measured.

Immunosuppressive assay

$CD45^+CD33^+CD14^+CD15^{-/dim}$ and $CD45^+CD33^+CD14^-CD15^{bright}$ MDSC subsets were sorted from breast tumor tissues. MDSCs were cultured with T cells (4×10^4) at different ratio in the presence of 2.5 μg/mL anti-human CD3 and 1.25 μg/mL anti-human CD28 for 3 days. T-cell proliferation was determined by Ki67 expression and CFSE dilution. T cell cytokine expression was evaluated by intracellular staining. The analysis was gated on $CD3^+$ T cells.

Lentiviral vector construction

MCF7 cells were transfected with GFP expressing lentiviral vectors encoding shSTAT3 (Supplementary Table 2) or nonfunctional scrambled control. After transfection, the transfected cells were selected and cultured for further experiments.

Flow cytometry analysis and cell sorting

Single cell suspensions were made from different organs and tumor tissues. Cells were labeled with fluorescence-conjugated antibodies to CD3, CD4, CD5, CD11b, CD14, CD15, CD16, CD19, CD33, CD45, HLA-DR, ALDH and STAT3 (BD Pharmingen). The cells were analyzed by LSR II (BD Biosciences, San Jose, CA). The primary cells were sorted from fresh tissues by high speed sorter ARIA (BD Biosciences, San Jose, CA).

Western blot analysis

Cell lysates were prepared with SDS lysis buffer and clarified by centrifugation, and protein concentration were determined by BCA protein assay kit (Thermo scientific). Equivalent amounts of total cellular proteins were separated by SDS PAGE, and transferred onto PVDF membranes. Proteins are detected with the antibodies against STAT3 and p-STAT3 (Y705) (Cell Signaling), NOTCH1 (Abcam), NICD (Cleaved NOTCH1 Val1744, Cell Signaling) and GAPDH (6C5, Santa Cruz Biotechnology). EMT associated proteins were detected with Epithelial-Mesenchymal Transition (EMT) proteins Antibody Sampler Kit (Cell Signaling).

Real-time reverse-transcriptase polymerase chain reaction (RT-PCR) and ELISA assay

Real-time PCR was performed as we described ([24,31]). All the primers were included in the supplementary information (Supplementary Table 2). Cytokine production was measured by ELISA as described by manufacturer's protocol (R&D DY206). Nitric Oxide was detected in cultured supernatant according to manufacturer's protocol (Total Nitric Oxide and Nitrate/Nitrite Parameter Assay Kit, R&D Systems, KGE001) and normalized to the medium control.

Tumor sphere formation

MDSCs were sorted from human breast tumor tissues by high-speed sorter (FACSAria, BD) as described ([13]). Sphere assay was performed as described ([24,32]). Briefly, tumor cells or sorted tumor cell subsets were plated in ultra-low attachment plates (Corning, MA) in serum-free EBM-2 or X-VIVO medium (Lonza) supplemented with 5 μg/mL insulin (Sigma), 20 ng/mL human recombinant epidermal growth factor (EGF; Invitrogen), at a density of 1,000–10,000 viable cells/well. Spheres (> 50μm) were counted after 1–6 weeks.

MDSC and tumor co-culture

Human breast cancer cells (10^6/ml) were co-cultured with MDSCs in transwell system with 3 μM Notch inhibitor, γ-secretase inhibitor I (Z-LLNLe-CHO; Calbiochem, San Diego, CA) or/and 500 nM STAT3 inhibitor (Cucurbitacin I, Calbiochem). Tumor cells were subjected to genetic and functional analyses.

Statistical analysis

The Wilcoxon signed-rank test was used to determine pairwise differences and the Mann–Whitney U test was used to determine differences between groups. $P < 0.05$ was considered as significant. All statistical analysis was done on Statistica software (StatSoft Inc., Tulsa, OK). Overall patient survival was measured from the date of diagnosis to tumor related death. Data were censored at the last follow-up for patients who were alive at the time of analysis. Spearman correlation coefficients were computed to assess relationships between MDSCs and ALDH. Survival curves were constructed using the method of Kaplan–Meier and survival differences were assessed using the log-rank test. The Cox proportional hazards model was used to assess the effect of MDSC infiltration after adjusting important prognostic factors, including cohort, histotype, tumor type, stage, grade and treatment. Statistical significance was defined as a p-value <0.05. All analyses were performed using SAS 9.3 software.

Results

MDSCS are functionally relevant in human breast cancer

We isolated myeloid cells from human breast cancer for the phenotypic, molecular, functional and clinical studies. Polychromatic flow cytometry analysis demonstrated that there existed substantial $CD45^+$ immune cell subsets including $CD19^+CD45^+$ cells, $CD5^+CD45^+$ cells and $CD5^-CD19^-CD33^+CD45^+$ cells in fresh breast cancer tissues (Fig. 1a). $CD5^-CD19^-CD33^+CD45^+$ cells expressed high levels of CD11b and low to medium

levels of CD14, CD15, CD16, and HLA-DR (Fig. 1b, c). There were 22% of lin$^-$CD33$^+$CD11b$^+$CD45$^+$ cells in total CD45$^+$ immune cells in fresh breast cancer tissues (Fig. 1d). The lin$^-$CD33$^+$CD11b$^+$CD45$^+$ cells were sorted by high speed sorter to high purity (>97%) and were subjected to a suppression assay. These cells suppressed T cell proliferation as shown by reduced Ki67 expression in T cells (Fig. 1e), decreased CFSE-labeled T cell divisions (Fig. 1f) and effector T cells (Fig. 1g). The percentages of CD14$^+$CD15$^{-/dim}$ cells were higher than that of CD14$^-$CD15^{high} cells (Fig. 1c) and the two subsets were capable of inhibiting T cell proliferation (Supplementary Fig. 1b). Based on the phenotype and immune suppressive capacity, lin$^-$CD33$^+$CD11b$^+$CD45$^+$ cells are referred as myeloid derived suppressor cells (MDSCs).

MDSCS are clinically relevant in human breast cancer

Given the high levels of CD33 expression on MDSCs, we attempted to quantify MDSCs with CD33 in the paraffin-fixed breast cancer tissues. When we stained single cells from fresh breast cancer tissue cells with anti-CD33 (Supplementary Fig. 1a), we found that CD33^{high} cells were basically confined to CD3$^-$CD19$^-$CD45$^+$ cells (Supplementary Fig. 1a). Thus, CD33 may be an operational marker to phenotypically define MDSCs in paraffin-fixed breast cancer tissues. We quantified CD33$^+$ cells with immunohistochemical staining (IHC) in three patient cohorts (Supplementary Table 1). The European patient cohort 1 (cohort 1) included 104 treatment-naïve Her-2/neu$^+$ primary breast cancer patients. The Michigan patient cohort (cohort 2) and the Poland patient cohort 3 (cohort 3) included 84 and 90 breast cancer patients respectively, regardless of their Her-2/neu status (Supplementary Table 1). We observed that the levels of CD33$^+$ cells were variable from patient to patient (Fig. 2a). However, the levels of CD33$^+$ cells were comparable among 3 cohorts (Supplementary Fig. 2). For survival analyses, similar to our tumor associated regulatory T cell analysis ([29]), we summed the three cohorts and divided the patients into high and low groups based on the median levels of CD33$^+$ cells.

Kaplan-Meier analyses indicated that high levels of CD33$^+$ cells correlated with reduced overall survival compared to low levels of CD33$^+$ cells in the total patient population in univariate analysis (Fig. 2b, Supplementary Table 1). As patients in cohort 1 were exclusively Her2$^+$, to avoid potential bias due to patient distribution, we independently analyzed the cohort 1 and the combined cohorts 2 and 3. We found that high levels of CD33$^+$ cells were associated with reduced overall survival compared to low levels of CD33$^+$ cells in the cohort 1 (Fig. 2c) and the combined cohorts 2 and 3 (Fig. 2d). In a multivariate analysis including covariates of cohorts, histology, tumor type, stage, treatment and grade, high MDSC infiltration was again associated with shorter survival in all the 3 cohorts (Supplementary Table 3), the cohort 1 (Supplementary Table 4) and the combined cohorts 2 and 3 (Supplementary Table 5). Thus, MDSCs are functionally and clinically important in patients with breast cancer.

MDSCs induce human breast CSCs

Next we investigated the mechanisms by which MDSCs are associated with poor patient outcome. CSCs contribute to tumor progression and therapeutic resistance ([7,8,33]). We reasoned that MDSCs might affect CSC biological behavior. We showed that human breast

cancer associated MDSCs promoted MCF-7 breast cancer sphere formation (Fig. 3a). ALDH-1$^+$ cells are enriched with CSCs in breast and ovarian cancer cells ([24,34]). We observed that MDSCs enhanced human breast ALDH$^+$ cells (Fig. 3b), stimulated multiple core stem cell gene expression (Fig. 3c), but have no effect on cancer cell proliferation (Supplementary Fig. 3a). To test if MDSCs were directly associated with CSCs in patients with breast cancer, we quantified ALDH$^+$ CSCs in human breast cancer tissues. Breast cancer cells expressed a variety of ALDH levels (Supplementary Fig. 3b). The median levels of CD33$^+$ cells (MDSCs) positively correlated with that of ALDH$^+$ CSCs (Fig. 3d). Similar results were observed in the cohort 1 (Supplementary Fig. 3c) and cohort 2 (Supplementary Fig. 3b), respectively. Finally we evaluated the relevance of the interaction between MDSCs and tumor cells in the human xenograft model. Human cancer MDSCs were co-injected with MCF7 breast cancer cells into in female NOD-scid IL2Rγ null (NSG) mice. We found that MDSCs accelerated tumor progression (Fig. 3e). Furthermore, MDSCs increased the incidence of breast cancer tumor formation in NSG model (Fig. 3f). Cancer stemness is often associated with epithelial–mesenchymal transition (EMT). We found that MDSCs increased EMT-related gene expression as shown by Western blotting (Supplementary Fig. 3e) and immunofluorescence staining (Supplementary Fig. 3f). The data support a role of MDSCs in human breast cancer in vivo. Thus, MDSCs are biologically and clinically linked to breast cancer stemness.

MDSCs induce human breast CSCs through STAT3 and NOTCH signaling

STAT3 ([18,20–23]) and NOTCH ([20,35,36]) activation is observed in a variety of cancers and may control cancer progression and metastasis. We found that MDSCs strongly induced STAT3 phosphorylation in MCF-7 and MDA-MB-231 breast cancer cells co-cultured with MDSCs (Fig. 4a). Interestingly, NOTCH was also activated in MCF-7 breast cancer cells by MDSCs as shown by high expression of NOTCH2, NOTCH3, CHERP, HEY1 and HEY2 transcripts (Fig. 4b) and of intracellular domain of NOTCH (NICD) expression (Fig. 4c). MDSCs promoted breast cancer stemness and were associated with the levels of ALDH$^+$ breast cancer stem cells in breast cancer tissues (Fig. 3). We hypothesized that STAT3 and NOTCH activation was involved in MDSC-stimulated breast cancer stemness. To test this hypothesis, we blocked NOTCH and STAT3 signaling in human MDSC and breast cancer cell co-culture. The Notch inhibitor or the STAT3 inhibitor partially, and their combination completely, reduced ALDH$^+$ breast CSCs induced by MDSCs (Fig. 4d). The data indicate that MDSCs activate STAT3 and NOTCH, and induce human breast CSCs.

MDSC-derived IL-6 and NO mediate CSC induction

As MDSCs induced CSCs partially via STAT3 activation, we examined how MDSCs activated STAT3. IL-6 has been reported to activate STAT3 and was associated with tumorigenesis ([18,20–23]). Tumor associated CD14$^+$CD15$^{-/dim}$ MDSCs expressed high levels of IL-6 (Fig. 5a, Supplementary Fig. 4a). Breast cancer cells expressed IL-6 receptor (Supplementary Fig. 4b) and IL-6 activated STAT3 (Supplementary Fig. 4d). STAT3 inhibition partially suppressed breast CSCs induced by MDSCs (Fig. 4c). It suggests that MDSCs may promote CSCs via IL-6-mediated STAT3 activation.

As MDSCs induced CSCs partially through NOTCH activation, we further examined how MDSCs activated NOTCH. MDSCs may release reactive nitrogen intermediates to suppress immune responses ([37]). We detected high levels of nitric oxide (NO) in the culture supernatants of $CD14^{+}CD15^{-/dim}$ and $CD14^{-}CD15^{+}$ MDSCs (Fig. 5b, Supplementary Fig. 4c). GSNO stimulated NOTCH activation (Fig. 5c) and NOTCH gene expression (Fig. 5d).

Next we evaluated the relative impact of MDSC-derived IL-6 and NO on CSC induction. In the co-culture of breast cancer cells and MDSCs, anti-IL-6 mAb or iNOS inhibitor partially, and their combination completely, reduced sphere formation stimulated by MDSCs (Fig. 5e). Thus, our results suggest that MDSC-derived IL-6 and NO may collaboratively activate STAT3 and NOTCH, and induce breast CSCs.

STAT3 and NOTCH cooperatively support cancer stemness

Finally we investigated how MDSC-derived IL-6 and NO cooperatively activate STAT3 and NOTCH, and support cancer stemness. We first evaluated if STAT3 and NOTCH signaling reciprocally affected their counterpart's expression in the co-culture of MDSCs and breast cancer cells. Genetic knockdown of STAT3 with specific shSTAT3 abrogated the NOTCH activation mediated by MDSCs, as shown by reduced NICD expression (Fig. 6a), and whereas the inhibition of NOTCH with NOTCH inhibitor reduced STAT3 activation mediated by MDSCs (Fig. 6b). STAT3 inhibitor was included as a positive control (Fig. 6b).

We further examined the roles of NO and IL-6 in MDSC-mediated STAT3 activation and the kinetics of STAT3 phosphorylation. MDSCs mediated potent tumor STAT3 activation (Fig. 4a, Fig. 6a, b). This activation was partially reduced by iNOS inhibitors and anti-IL-6 mAb, and completely blocked by both iNOS inhibitor and anti-IL-6 mAb (Fig. 6c). The data raise the possibility that MDSCs induce potent STAT3 activation via IL-6-and NO-signaling collaboration in human breast cancers.

We further investigated the kinetics and persistence of STAT3 activation via IL-6 and NO interaction. We observed that STAT3 activation induced by IL-6 was faint within one hour (Fig. 6d). In contrast, addition of GSNO sustained and prolonged STAT3 activation (Fig 6d). Interestingly, GSNO potently activated NOTCH (Fig. 5c, d) and weakly stimulated STAT3 activation (Fig 6d). Thus, the data suggest that MDSC-derived NO activates NOTCH to facilitate and sustain persistent cancer STAT3 phosphorylation stimulated by MDSC-derived IL-6 and IL-6 may not be solely responsible for long-lasting STAT3 activation in tumor cells.

We tested the relevance of the interaction between MDSCs and tumor cells in the human xenograft model. Human cancer MDSCs were co-injected with MCF7 breast cancer cells into in female NOD-scid IL2Rγ null (NSG) mice. We found that MDSCs accelerated tumor progression. The effect was blocked by the treatment with anti-IL-6 and iNOS inhibitor (Fig. 6e). In line with this, we found that MDSCs increased ALDH1 expression in tumor cells and blockade of iNOS and IL-6 abolished this effect (Fig. 6f, g). Furthermore, we analyzed the correlations among *ALDH1A1, IL6* and *CD33* transcripts in TCGA breast cancer data (Oncomine.org). We observed strong correlations among *ALDH1A1, IL6* and *CD33*

transcripts (Supplementary Fig. 5). This data support a role of MDSCs and MDSC-derived IL6 and NO in human breast cancer progression in vivo.

Altogether, we have demonstrated that MDSC-derived IL-6 initiates STAT3 phosphorylation, MDSC-derived NO activates NOTCH, and NOTCH subsequently and collaboratively acts with IL-6 to promote prolonged STAT3 activation. Thus, MDSCs may play a role in stimulating and maintaining CSC pool through the interaction between IL-6/STAT3 and NO/NOTCH (Fig. 6h).

Discussion

In this study we have generated important novel insights into MDSC and cancer stem cell immunobiology and pathology in the context of human breast cancer. (i) MDSCs provide extrinsic signals for cancer stem cell renewal and promote tumor metastatic and tumorigenic potential. (ii) MDSCs impact cancer stem cell biology through IL-6/STAT3 and NO/NOTCH signaling pathways. (iii) NO/NOTCH signaling enforces and sustains persistent and potent IL-6/STAT3 activation, and affects cancer stemness. (iv) The interaction between MDSCs and cancer stem cells is biologically and clinically relevant in patients with breast cancer.

Immune suppressive effects of MDSCs are relatively well-studied in tumor bearing mouse models ([38]). Myeloid cells including MDSCs and macrophages have been linked with cancer stemness ([13],[39],[40]). However, the non-immunological effects of MDSCs are poorly understood in human breast cancer. It has been reported that peripheral blood MDSCs correlate with clinical cancer stage, metastatic tumor burden, and doxorubicin-cyclophosphamide chemotherapy ([41]). In line with this, we have found high numbers of MDSCs in breast cancer tissues. To our surprise, MDSCs directly promote and maintain the cancer stem cell pool through two integrated signaling pathways: IL-6/STAT3 and NO/NOTCH signaling pathways.

The link between IL-6 and STAT3 has been reported in several types of cancer ([18],[20_23]). Interestingly, IL-6 alone induces transient STAT3 phosphorylation, while MDSCs induce long-lasting STAT3 activation. MDSC-derived NO activates NOTCH and contributes to sustained STAT3 phosphorylation through IL-6 and NO collaborative action. In support of this, it has been demonstrated that NO stimulates NOTCH signaling and delivers a survival signal to glioma cells ([42]) and drosophila blood cells ([43]). Thus, although many factors can regulate NOTCH and STAT3 signaling pathways in cancer, our work support the notion that MDSCs integrate the signaling networks between NO/NOTCH and IL-6/STAT3 in breast cancer. We propose that MDSCs contribute to persistent and potent STAT3 activation in breast cancer, which promotes and maintains the CSC pool. Given the role of CSCs in cancer metastasis, our work also supports the notion that STAT3 signaling is crucial for myeloid cell colonization at future metastatic sites ([19]).

After deciphering the molecular and cellular importance of the cross-talk between MDSCs and tumor cells in cancer stem cells, we have further addressed the biological and clinical relevance of this cross-talk in patients with breast cancer. MDSCs correlate with CSCs content in the human breast cancer microenvironment, and are adversely associated with

patient survival. It has been reported that response to Herceptin ([44]) and chemotherapy ([45]) is in part regulated by immune components in tumor bearing mouse models. Given the relevance of CSCs in tumor relapse and therapy resistance ([7,8,33]), our data point toward a possibility that immune suppressive element, MDSCs, directly target the cancer stemness signaling pathway and may potentially affect cancer therapy. Altogether, our results suggest that anti-cancer therapy should simultaneously target host MDSCs and cancer (stem) cells to improve therapeutic efficiency and abrogate therapy resistance. We have shown that CD33 is an operational marker for human tumor associated MDSCs([13]). Targeting CD33 is considered a strategy to treat patients with acute promyelocytic leukemia ([46]). Therefore, targeting CD33 signaling may be an optional regimen to treat breast cancer patients.

Supplementary Material

Refer to Web version on PubMed Central for supplementary material.

Acknowledgments

We thank Daniel Hayes for fruitful discussion and intellectual support, and Deborah Postiff, Michelle Vinco, Jackline Barikdar and Ronald Craig in the Pathology Department for their technical assistance.

Support: This work was supported in part by research grants from the NIH/NCI R01 grants (W.Z) (CA123088, CA099985, CA193136 and CA152470) and the NIH through the University of Michigan's Cancer Center Support Grant (CA46592).

References

1. Dunn GP, Bruce AT, Ikeda H, Old LJ, Schreiber RD. Cancer immunoediting: from immunosurveillance to tumor escape. Nat Immunol. 2002; 3(11):991–998. [PubMed: 12407406]
2. Yang X, Mortenson ED, Fu YX. Targeting and utilizing primary tumors as live vaccines: changing strategies. Cell Mol Immunol. 2012; 9(1):20–26. [PubMed: 22101245]
3. Koebel CM, Vermi W, Swann JB, Zerafa N, Rodig SJ, Old LJ, et al. Adaptive immunity maintains occult cancer in an equilibrium state. Nature. 2007; 450(7171):903–907. [PubMed: 18026089]
4. Pardoll DM. The blockade of immune checkpoints in cancer immunotherapy. Nat Rev Cancer. 2012; 12(4):252–264. [PubMed: 22437870]
5. Zou W. Immunosuppressive networks in the tumour environment and their therapeutic relevance. Nat Rev Cancer. 2005; 5(4):263–274. [PubMed: 15776005]
6. Wicha MS, Liu S, Dontu G. Cancer stem cells: an old idea--a paradigm shift. Cancer Res. 2006; 66(4):1883–1890. discussion 95–6. [PubMed: 16488983]
7. Dean M, Fojo T, Bates S. Tumour stem cells and drug resistance. Nat Rev Cancer. 2005; 5(4):275–284. [PubMed: 15803154]
8. Brabletz T, Jung A, Spaderna S, Hlubek F, Kirchner T. Opinion: migrating cancer stem cells - an integrated concept of malignant tumour progression. Nat Rev Cancer. 2005; 5(9):744–749. [PubMed: 16148886]
9. Hanahan D, Weinberg RA. The hallmarks of cancer. Cell. 2000; 100(1):57–70. [PubMed: 10647931]
10. Karnoub AE, Dash AB, Vo AP, Sullivan A, Brooks MW, Bell GW, et al. Mesenchymal stem cells within tumour stroma promote breast cancer metastasis. Nature. 2007; 449(7162):557–563. [PubMed: 17914389]
11. Katoh H, Wang D, Daikoku T, Sun H, Dey SK, Dubois RN. CXCR2-Expressing Myeloid-Derived Suppressor Cells Are Essential to Promote Colitis-Associated Tumorigenesis. Cancer Cell. 2013; 24(5):631–644. [PubMed: 24229710]

12. Balkwill F, Mantovani A. Inflammation and cancer: back to Virchow? Lancet. 2001; 357(9255): 539–545. [PubMed: 11229684]
13. Cui TX, Kryczek I, Zhao L, Zhao E, Kuick R, Roh MH, et al. Myeloid-derived suppressor cells enhance stemness of cancer cells by inducing microRNA101 and suppressing the corepressor CtBP2. Immunity. 2013; 39(3):611–621. [PubMed: 24012420]
14. DeNardo DG, Barreto JB, Andreu P, Vasquez L, Tawfik D, Kolhatkar N, et al. CD4(+) T cells regulate pulmonary metastasis of mammary carcinomas by enhancing protumor properties of macrophages. Cancer Cell. 2009; 16(2):91–102. [PubMed: 19647220]
15. Kryczek I, Lin Y, Nagarsheth N, Peng D, Zhao L, Zhao E, et al. IL-22(+)CD4(+) T cells promote colorectal cancer stemness via STAT3 transcription factor activation and induction of the methyltransferase DOT1L. Immunity. 2014; 40(5):772–784. [PubMed: 24816405]
16. Kim S, Takahashi H, Lin WW, Descargues P, Grivennikov S, Kim Y, et al. Carcinoma-produced factors activate myeloid cells through TLR2 to stimulate metastasis. Nature. 2009; 457(7225):102–106. [PubMed: 19122641]
17. Qian BZ, Li J, Zhang H, Kitamura T, Zhang J, Campion LR, et al. CCL2 recruits inflammatory monocytes to facilitate breast-tumour metastasis. Nature. 2011; 475(7355):222–225. [PubMed: 21654748]
18. Yu H, Kortylewski M, Pardoll D. Crosstalk between cancer and immune cells: role of STAT3 in the tumour microenvironment. Nat Rev Immunol. 2007; 7(1):41–51. [PubMed: 17186030]
19. Deng J, Liu Y, Lee H, Herrmann A, Zhang W, Zhang C, et al. S1PR1-STAT3 signaling is crucial for myeloid cell colonization at future metastatic sites. Cancer Cell. 2012; 21(5):642–654. [PubMed: 22624714]
20. Sansone P, Storci G, Tavolari S, Guarnieri T, Giovannini C, Taffurelli M, et al. IL-6 triggers malignant features in mammospheres from human ductal breast carcinoma and normal mammary gland. J Clin Invest. 2007; 117(12):3988–4002. [PubMed: 18060036]
21. Gao SP, Mark KG, Leslie K, Pao W, Motoi N, Gerald WL, et al. Mutations in the EGFR kinase domain mediate STAT3 activation via IL-6 production in human lung adenocarcinomas. J Clin Invest. 2007; 117(12):3846–3856. [PubMed: 18060032]
22. Grivennikov S, Karin E, Terzic J, Mucida D, Yu GY, Vallabhapurapu S, et al. IL-6 and Stat3 are required for survival of intestinal epithelial cells and development of colitis-associated cancer. Cancer Cell. 2009; 15(2):103–113. [PubMed: 19185845]
23. Marotta LL, Almendro V, Marusyk A, Shipitsin M, Schemme J, Walker SR, et al. The JAK2/STAT3 signaling pathway is required for growth of CD44(+)CD24(−) stem cell-like breast cancer cells in human tumors. J Clin Invest. 2011; 121(7):2723–2735. [PubMed: 21633165]
24. Kryczek I, Liu S, Roh M, Vatan L, Szeliga W, Wei S, et al. Expression of aldehyde dehydrogenase and CD133 defines ovarian cancer stem cells. Int J Cancer. 2012; 130(1):29–39. [PubMed: 21480217]
25. Kryczek I, Lin Y, Nagarsheth N, Peng D, Zhao L, Zhao E, et al. IL-22CD4 T Cells Promote Colorectal Cancer Stemness via STAT3 Transcription Factor Activation and Induction of the Methyltransferase DOT1L. Immunity. 2014
26. Crown JP, Dieras V, Staroslawska E, Yardley DA, Bachelot T, Davidson N, et al. Phase III trial of sunitinib in combination with capecitabine versus capecitabine monotherapy for the treatment of patients with pretreated metastatic breast cancer. Journal of clinical oncology : official journal of the American Society of Clinical Oncology. 2013; 31(23):2870–2878. [PubMed: 23857972]
27. Janni W, Sarosiek T, Karaszewska B, Pikiel J, Staroslawska E, Potemski P, et al. A phase II, randomized, multicenter study evaluating the combination of lapatinib and vinorelbine in women with ErbB2 overexpressing metastatic breast cancer. Breast cancer research and treatment. 2014; 143(3):493–505. [PubMed: 24402830]
28. Curiel TJ, Wei S, Dong H, Alvarez X, Cheng P, Mottram P, et al. Blockade of B7-H1 improves myeloid dendritic cell-mediated antitumor immunity. Nat Med. 2003; 9(5):562–567. [PubMed: 12704383]
29. Curiel TJ, Coukos G, Zou L, Alvarez X, Cheng P, Mottram P, et al. Specific recruitment of regulatory T cells in ovarian carcinoma fosters immune privilege and predicts reduced survival. Nat Med. 2004; 10(9):942–949. [PubMed: 15322536]

30. Kryczek I, Zou L, Rodriguez P, Zhu G, Wei S, Mottram P, et al. B7-H4 expression identifies a novel suppressive macrophage population in human ovarian carcinoma. J Exp Med. 2006; 203(4): 871–881. [PubMed: 16606666]
31. Kryczek I, Zhao E, Liu Y, Wang Y, Vatan L, Szeliga W, et al. Human TH17 Cells Are Long-Lived Effector Memory Cells. Sci Transl Med. 2011; 3(104):104ra00.
32. Liu S, Ginestier C, Charafe-Jauffret E, Foco H, Kleer CG, Merajver SD, et al. BRCA1 regulates human mammary stem/progenitor cell fate. Proc Natl Acad Sci U S A. 2008; 105(5):1680–1685. [PubMed: 18230721]
33. Pardal R, Clarke MF, Morrison SJ. Applying the principles of stem-cell biology to cancer. Nat Rev Cancer. 2003; 3(12):895–902. [PubMed: 14737120]
34. Ginestier C, Hur MH, Charafe-Jauffret E, Monville F, Dutcher J, Brown M, et al. ALDH1 is a marker of normal and malignant human mammary stem cells and a predictor of poor clinical outcome. Cell Stem Cell. 2007; 1(5):555–567. [PubMed: 18371393]
35. Choi JH, Park JT, Davidson B, Morin PJ, Shih Ie M, Wang TL. Jagged-1 and Notch3 juxtacrine loop regulates ovarian tumor growth and adhesion. Cancer Res. 2008; 68(14):5716–5723. [PubMed: 18632624]
36. Cancer Genome Atlas Research N. Integrated genomic analyses of ovarian carcinoma. Nature. 2011; 474(7353):609–615. [PubMed: 21720365]
37. Kusmartsev SA, Li Y, Chen SH. Gr-1+ myeloid cells derived from tumor-bearing mice inhibit primary T cell activation induced through CD3/CD28 costimulation. J Immunol. 2000; 165(2): 779–785. [PubMed: 10878351]
38. Gabrilovich DI, Nagaraj S. Myeloid-derived suppressor cells as regulators of the immune system. Nat Rev Immunol. 2009; 9(3):162–174. [PubMed: 19197294]
39. Panni RZ, Sanford DE, Belt BA, Mitchem JB, Worley LA, Goetz BD, et al. Tumor-induced STAT3 activation in monocytic myeloid-derived suppressor cells enhances stemness and mesenchymal properties in human pancreatic cancer. Cancer Immunol Immunother. 2014; 63(5):513–528. [PubMed: 24652403]
40. Wan S, Zhao E, Kryczek I, Vatan L, Sadovskaya A, Ludema G, et al. Tumor-associated macrophages produce interleukin 6 and signal via STAT3 to promote expansion of human hepatocellular carcinoma stem cells. Gastroenterology. 2014; 147(6):1393–1404. [PubMed: 25181692]
41. Diaz-Montero CM, Salem ML, Nishimura MI, Garrett-Mayer E, Cole DJ, Montero AJ. Increased circulating myeloid-derived suppressor cells correlate with clinical cancer stage, metastatic tumor burden, and doxorubicin-cyclophosphamide chemotherapy. Cancer Immunol Immunother. 2009; 58(1):49–59. [PubMed: 18446337]
42. Charles N, Ozawa T, Squatrito M, Bleau AM, Brennan CW, Hambardzumyan D, et al. Perivascular nitric oxide activates notch signaling and promotes stem-like character in PDGF-induced glioma cells. Cell Stem Cell. 2010; 6(2):141–152. [PubMed: 20144787]
43. Mukherjee T, Kim WS, Mandal L, Banerjee U. Interaction between Notch and Hif-alpha in development and survival of Drosophila blood cells. Science. 2011; 332(6034):1210–1213. [PubMed: 21636775]
44. Park S, Jiang Z, Mortenson ED, Deng L, Radkevich-Brown O, Yang X, et al. The therapeutic effect of anti-HER2/neu antibody depends on both innate and adaptive immunity. Cancer Cell. 2010; 18(2):160–170. [PubMed: 20708157]
45. Denardo DG, Brennan DJ, Rexhepaj E, Ruffell B, Shiao SL, Madden SF, et al. Leukocyte Complexity Predicts Breast Cancer Survival and Functionally Regulates Response to Chemotherapy. Cancer Discov. 2011; 1:54–67. [PubMed: 22039576]
46. Walter RB, Appelbaum FR, Estey EH, Bernstein ID. Acute myeloid leukemia stem cells and CD33-targeted immunotherapy. Blood. 2012; 119(26):6198–6208. [PubMed: 22286199]

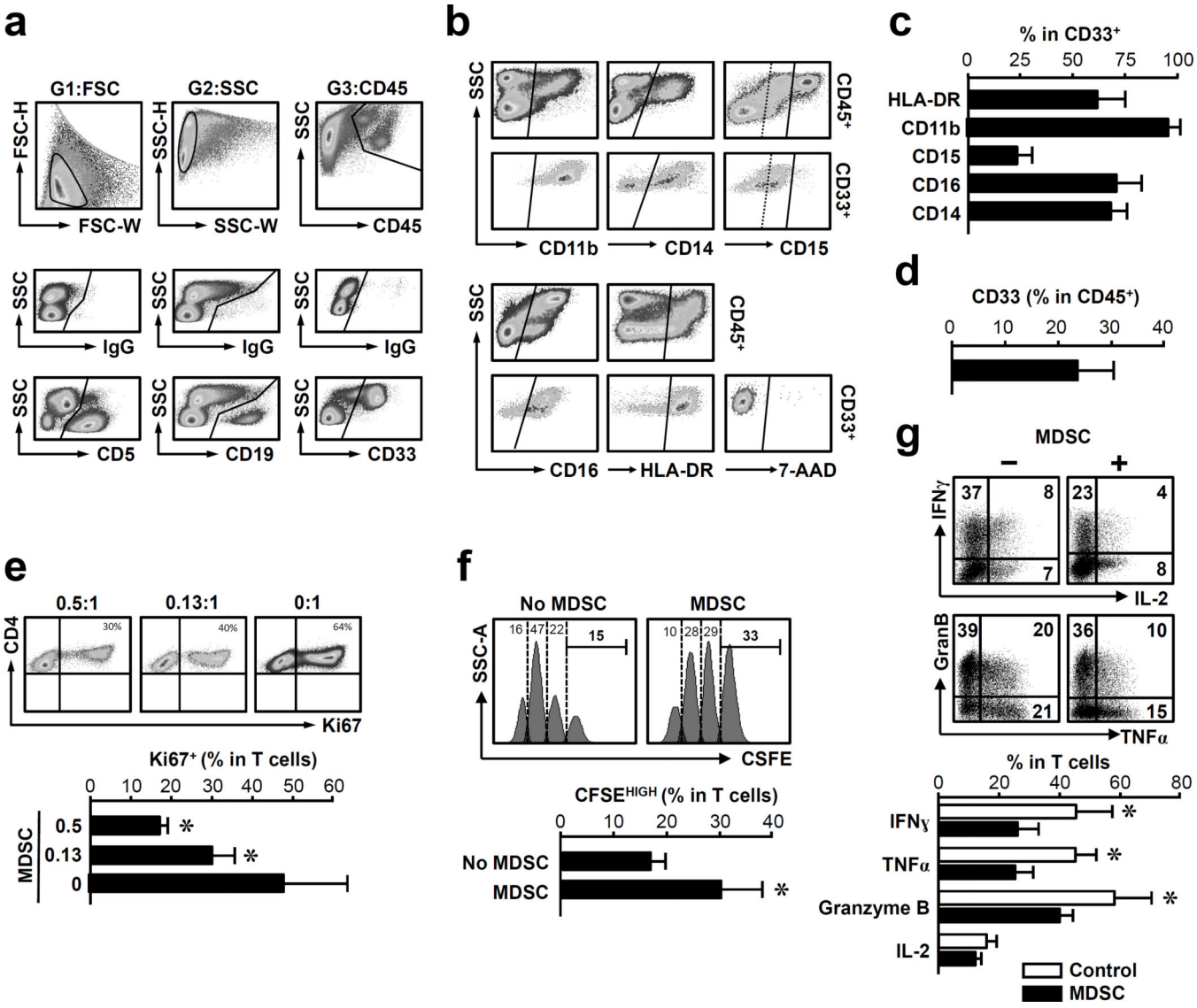

Figure 1. MDSCs are functionally relevant in human breast cancer

(**a–d**) Phenotype of MDSCs. Fresh breast cancer tissues were separated into single cell suspension. The cells were stained with isotype control antibodies and relevant antibodies. Polychromatic flow cytometry analysis was performed on these cells by gating on single cells in different gates (G1–G3). (**a**) The relationship among $CD45^+$, $CD5^+$, $CD19^+$ and $CD33^+$ cells. Upper panels: FSC, SSC, and CD45 gates; Middle panels: isotype controls in gates 1*2*3. Lower panels: CD19, CD5 and CD33 in gates 1*2*3; (**b**) The phenotype of MDSCs. The expression of CD11b, CD14, CD15, CD16, HLA-DR and 7-AAD was analyzed in $CD5^-CD19^-CD33^+CD45^+$ cells. (**c**) The percentage of different antigen expressing cells in $CD5^-CD19^-CD33^+CD45^+$ cells. (**d**) The percentage of CD33 expressing cells in $CD45^+$ cells. One of 10 representative patients is shown (**a, b**). Columns represent the mean ± SEM (**c, d**) (n = 10).

(**e–g**) MDSCs suppressed T cell activation. $CD3^+$ T cells were activated with anti-CD3 in the presence of MDSCs. (**e**) T cells were cultured with MDSCs at different ratio (MDSC: T

cell) for 48 hours. $Ki67^{+}CD3^{+}$ T cells were measured by flow cytometry. n = 3. (**f**) T cells were labeled with CFSE, and subsequently cultured with MDSCs. The $CD3^{+}$ T cell divisions were analyzed by FACS on day 10. (**g**) Effector molecules were detected in $CD3^{+}$ T cells by intracellular staining and analyzed by FACS. MDSC: T cell ratio was 0.5:1 (**f, g**). n = 4, *P < 0.03, Wilcoxon pair test.

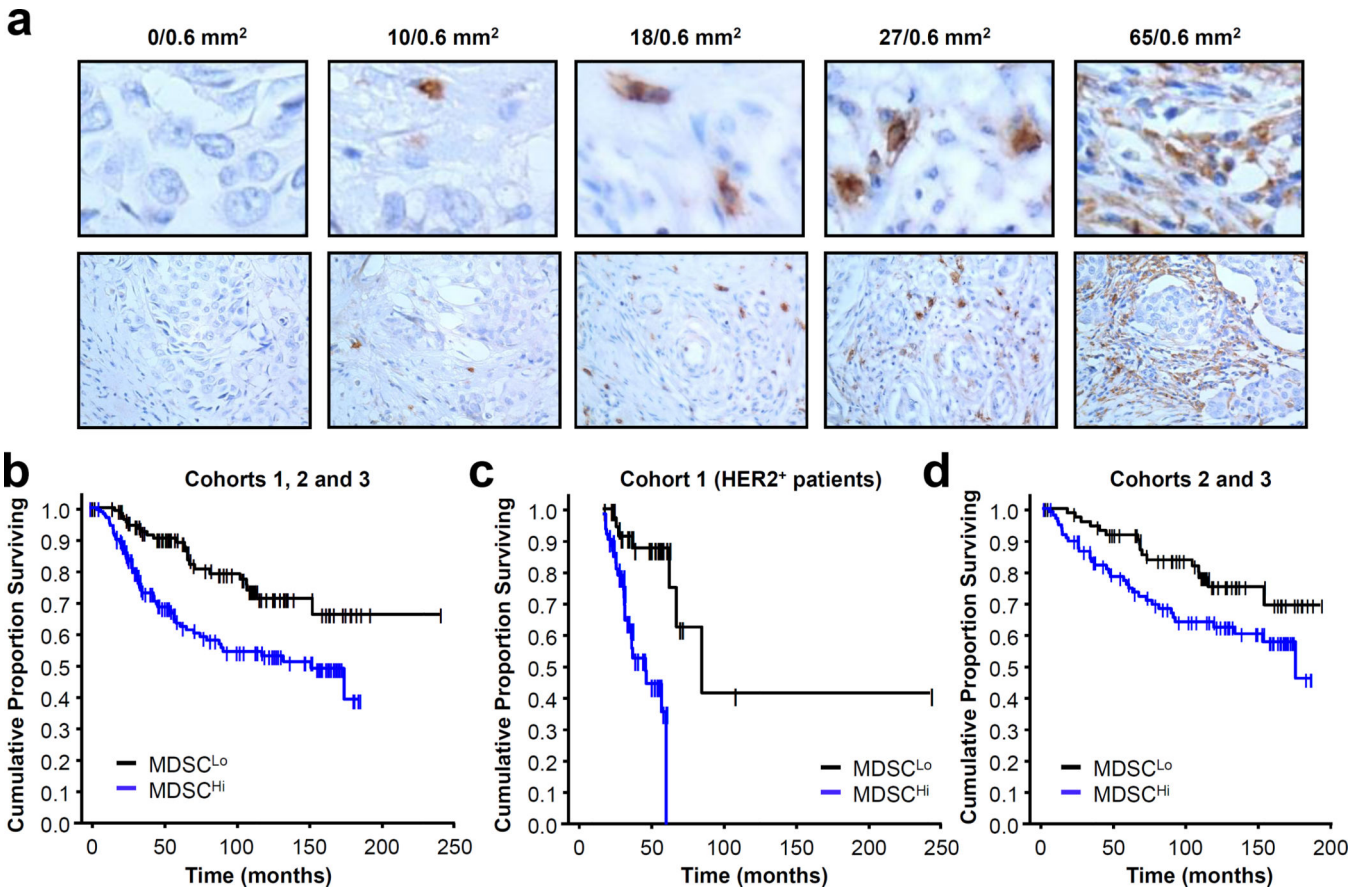

Figure 2. MDSCs are clinically relevant in human breast cancer

Immunohistochemistry was performed in human breast tumor tissues. $CD33^+$ cells were quantified in $0.6mm^2$.

(a) 5 representative cases with different levels of $CD33^+$ cell infiltration are shown. Upper panel, 40×; lower panel, 20×.

(**b–d**) Relationship between MDSCs and patient outcome. Breast cancer patients were divided into high and low $CD33^+$ cell infiltration based on the median value of CD33 expression (see Methods). Kaplan-Meier curves were drown based on the overall survival of all the 3-cohorts (n = 278, P < 0.01, log-rank test) (**b**) or the cohort 1 (N = 104, P = 0.01, log-rank test) (**c**) or the combined cohorts 2 and 3 (N = 174, P < 0.01, log-rank test) (**d**).

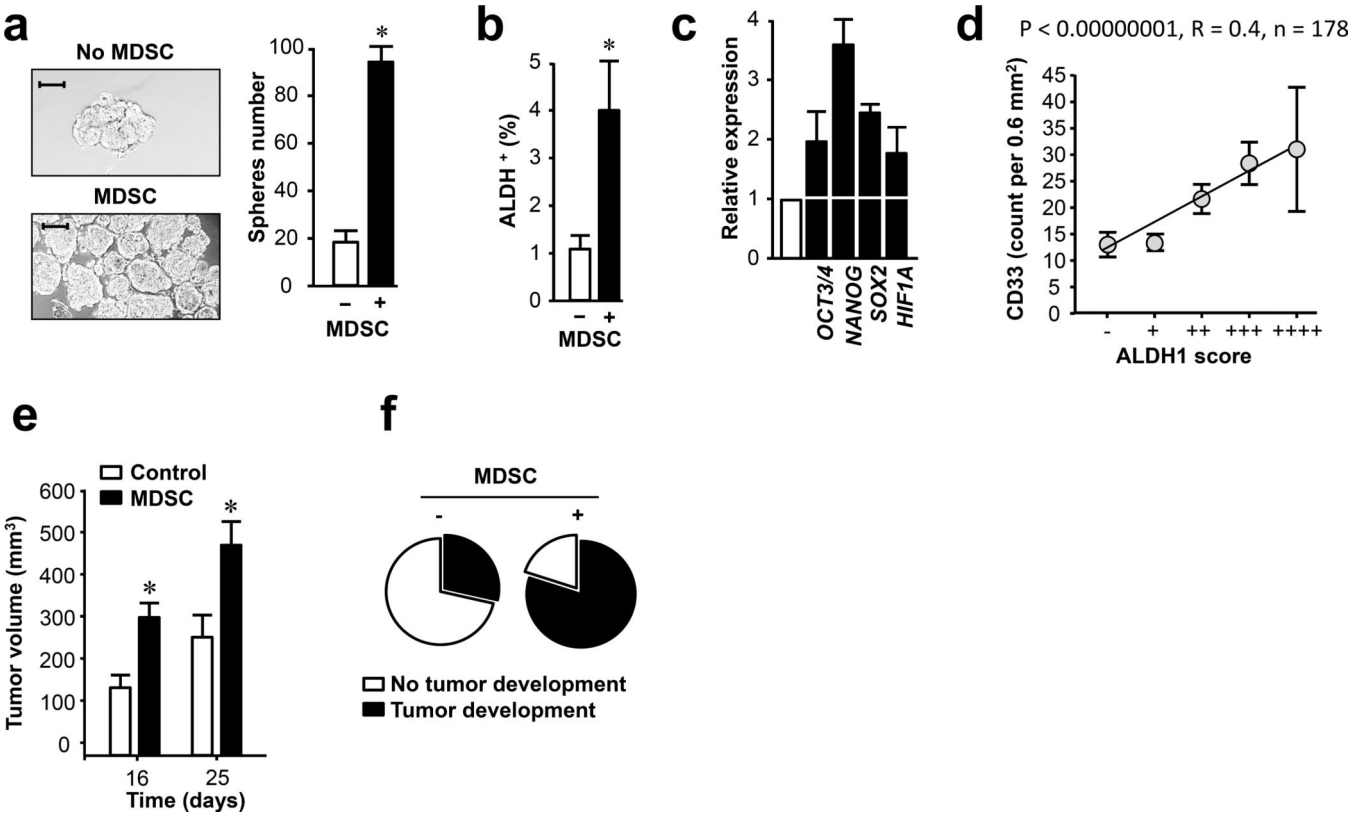

Figure 3. MDSCs promote and correlate human breast cancer stem cells

(**a**) Human MDSCs increased breast cancer sphere formation. Human MCF-7 breast cancer cells were cultured with MDSCs in sphere forming condition ([24]). Numbers of spheres are expressed as Mean ± SEM, n = 4, MDSCs derived from 3 different patients. *, P<0.05, Wilcoxon pair test.

(**b**) Human MDSCs increased $ALDH^+$ breast cancer stem cells. MCF-7 breast cancer cells and MDSCs were co-cultured in sphere forming condition ([24]). $ALDH^+$ cells were determined by FACS gated on $CD33^-$ tumor cells. Results are expressed as Mean ± SEM, triplicates with MDSCs derived from 3 different patients. *, P<0.05, Wilcoxon pair test.

(**c**) Human MDSCs stimulated human breast cancer stem cell core gene transcripts. MCF-7 cells were co-cultured with primary MDSCs in transwell for 48 hours. Stem cell core genes quantified by real-time PCR. Results are expressed as the mean relative values ± SD. Experiments were triplicates with MDSCs from 3 different patients.

(**d**) Relationship between MDSCs and $ALDH\text{-}1^+$ cancer stem cells in breast cancer tissues. $CD33^+$ cells and $ALDH\text{-}1^+$ tumor cells were evaluated by immunohistochemistry staining in tissues obtained from patients of cohorts 1 and 2. $CD33^+$ cells were quantified as the numbers of $CD33^+$ cells/0.6mm^2 in TMAs. $ALDH\text{-}1^+$ cells were scored from 0 to 4 based on the intensity of ALDH-1 expression (see Methods). Their correlation was analyzed by Pearson correlation. N = 178; P < 0.00000001, R = 0.4.

(**e**) Effects of MDSCs on human MCF-7 breast tumor growth in NSG mice. Human breast cancer MCF7 cells were mixed with MDSCs and inoculated subcutaneously into NSG mice supplied with E2 (estradiol-17β pellet). Tumor growth was monitored. N = 5/group; *, P < 0.05 (Wilcoxon pair test).

(f). Effects of MDSCs on human MCF-7 incidences in NSG mice. 10^5 MCF7 cells were mixed with MDSCs and inoculated subcutaneously into NSG mice supplied with E2 (estradiol-17β pellet). Tumor incidence was monitored for 16 days. N = 5/group.

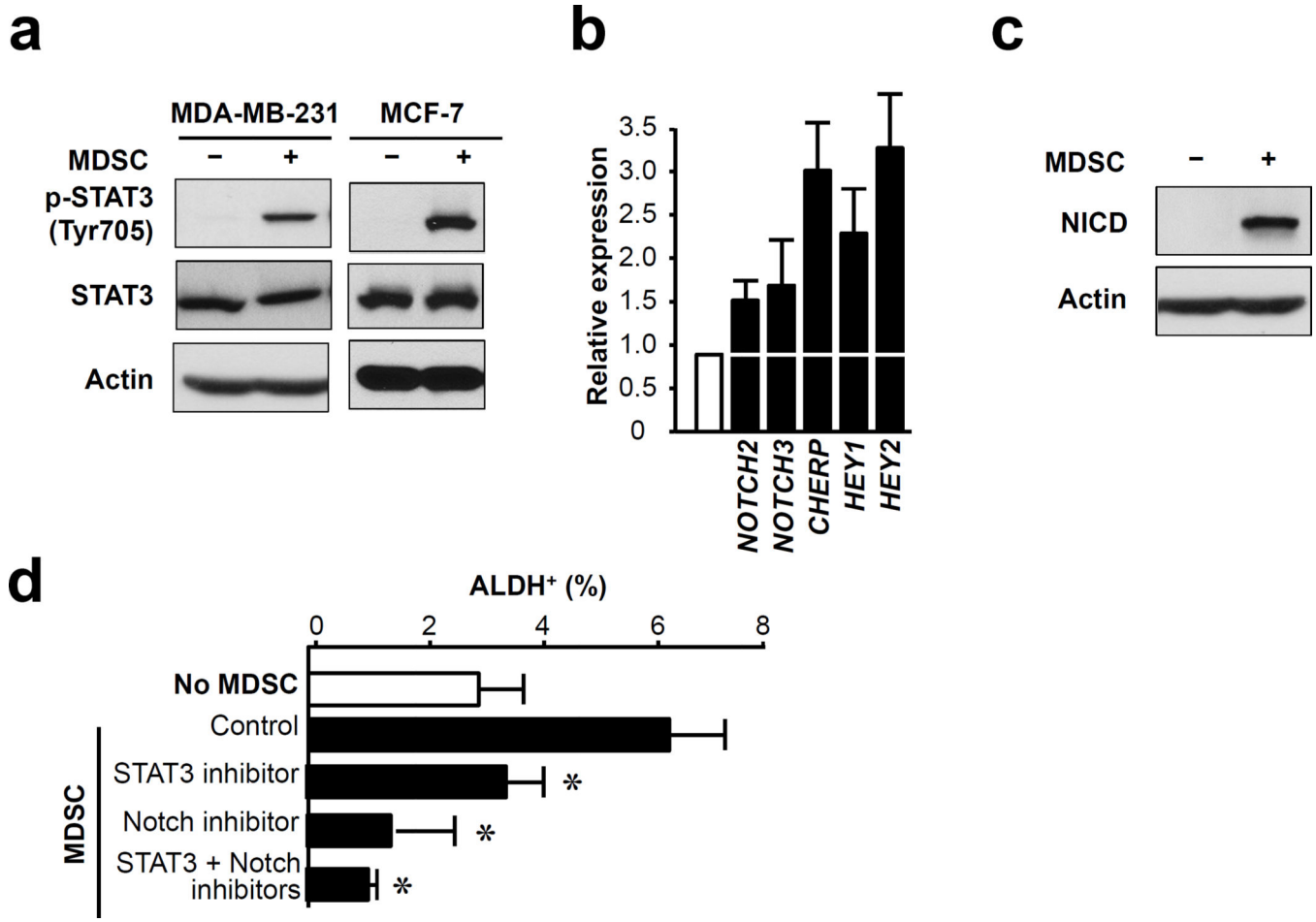

Figure 4. MDSCs induce CSCs through STAT3 and NOTCH signaling pathway

(**a**) Effects of MDSCs on STAT3 activation in MDA-231 and MCF-7 tumor cells. Tumor cells were co-cultured with MDSCs in transwell system, and STAT3 phosphorylation in tumor cells was detected by Western blot. One of 3 experiments is shown.

(**b, c**) Effects of MDSCs on NOTCH signaling activation in MCF-7. Tumor cells were co-cultured with MDSCs in transwell system. Expression of tumor Notch signaling transcripts was quantified by real-time PCR on day 1 (**b**) and cleaved NOTCH (NICD) was detected by Western blot on day 3. (**c**)

(**d**) Effects of biochemical inhibition of STAT3 and NOTCH on MDSC-induced human $ALDH^+$ breast cells. Human breast cancer cells were co-cultured with MDSCs in the presence of Notch inhibitor or STAT3 inhibitor. Human $ALDH^+$ breast cancer stem cells were analyzed by FACS. Results are expressed as the percentage of $ALDH^+$ cells ± SD. n = 4. *, $P<0.05$ (Wilcoxon pair test) in comparison to the control (MDSCs).

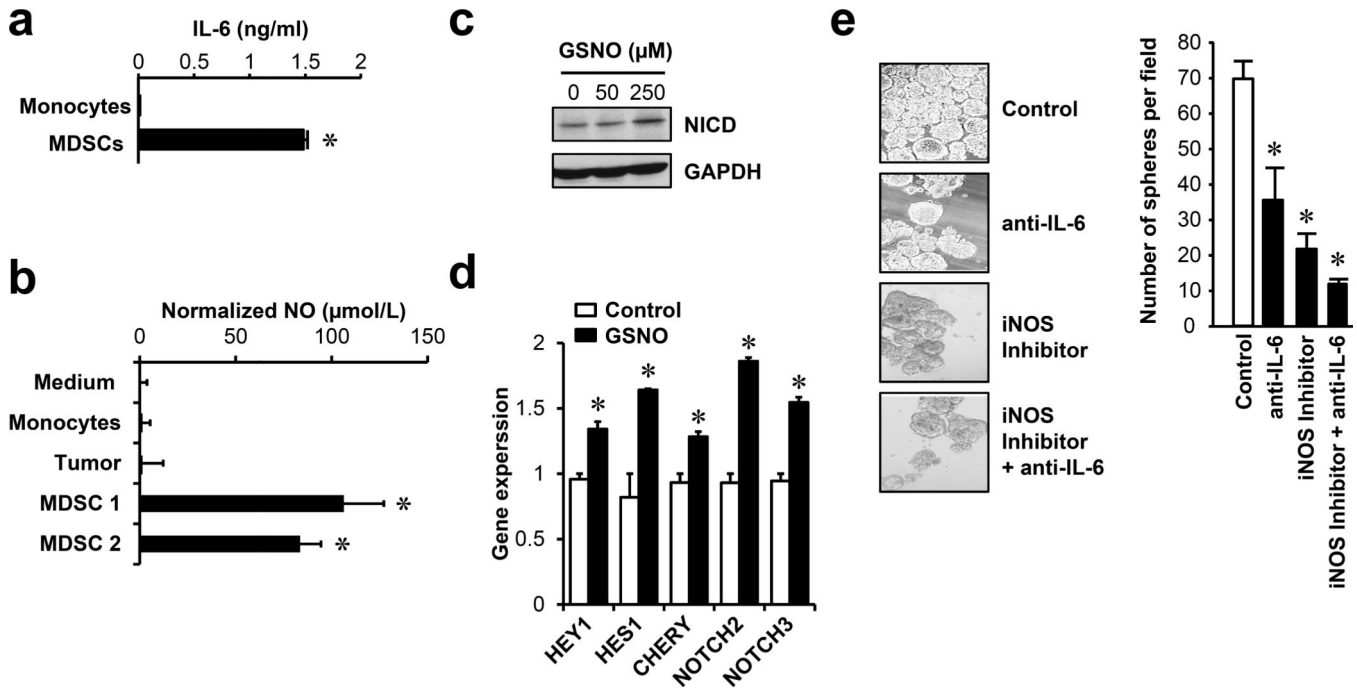

Figure 5. MDSC-derived IL-6 and NO mediate CSC induction

(**a, b**) IL-6 and NO released by MDSCs. Breast cancer-associated MDSCs were cultured for 2–3 days. IL-6 (**a**) and NO (**b**) were detected in the supernatants and normalized to medium. Results are expressed as the mean values ± SEM. Two independent experiments (MDSC1 and 2) with triplicates. P <0.05.

(**c–d**) Effects of GSNO on NOTCH signaling. MCF-7 tumor cells were cultured with GSNO for 3 days. NICD was detected by Western blot (**c**), and NOTCH associated gene expression was analyzed by real time PCR (**d**). Results are expressed as the mean ± SEM. N = 4, P <0.05.

(**e**) Effects of IL-6 and NO on human MDSC-induced breast cancer sphere formation. Human MCF-7 breast cancer cell sphere assay was performed for 10–15 days with MDSCs in the presence of anti-IL-6 mAb and iNOS inhibitors. One of 4 experiments is shown.

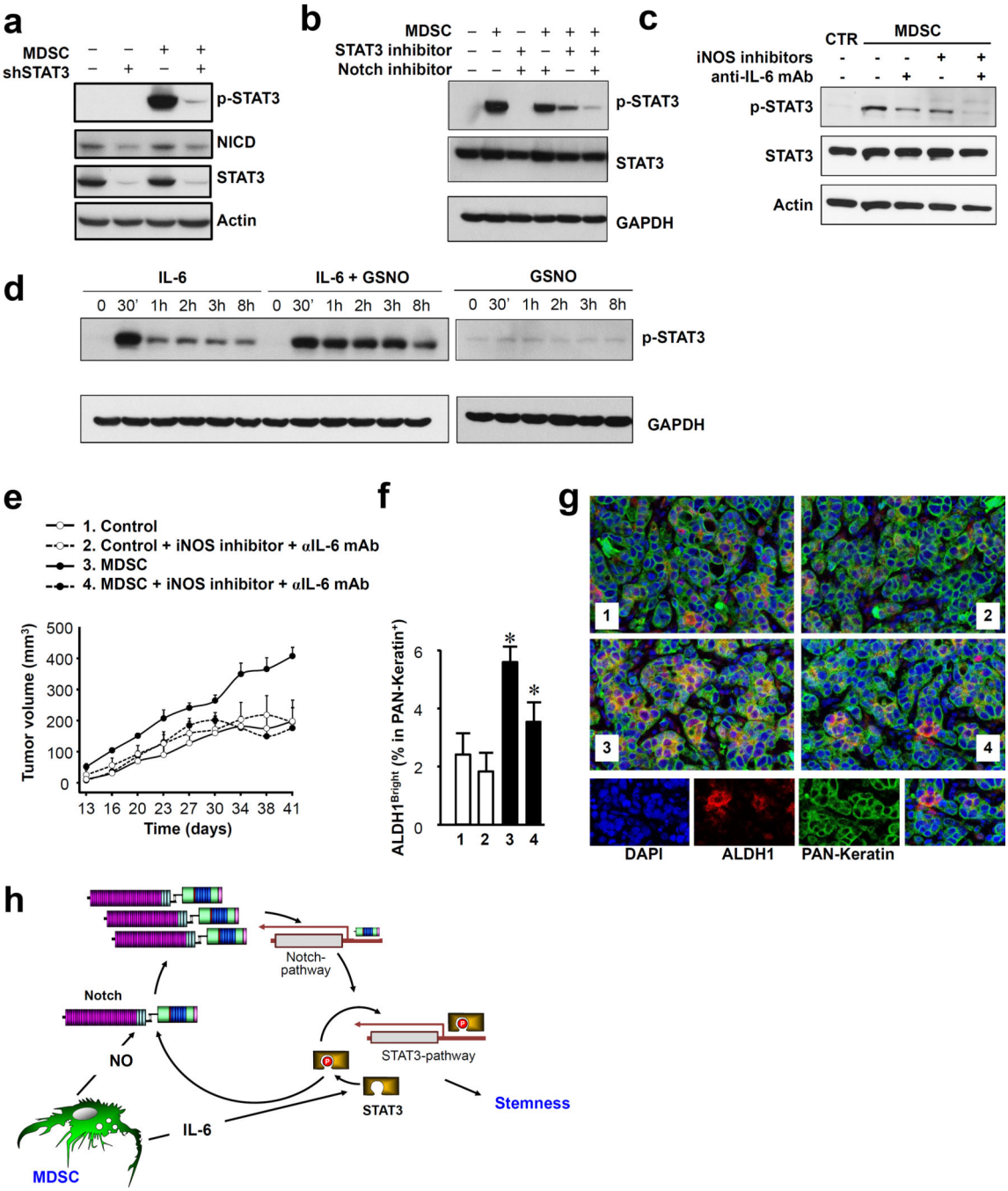

Figure 6. Activation of STAT3 and NOTCH supports cancer stemness

(**a**) Effects of shSTAT3 on MDSC-mediated NOTCH activation in MCF-7 cells. MCF-7 cells were cultured with MDSCs for 24 hours in transwell system. Active domain of NOTCH (NICD) was detected by Western blot.

(**b**) Effects of biochemical inhibition of NOTCH and STAT3 on MDSC-mediated STAT3 activation in breast cancer cells. MDA-231 cells were cultured with MDSCs for 24 hours in transwell system in the presence of STAT3 inhibitor (Cucurbitacin I) or NOTCH inhibitor (γ-secretase inhibitor I). STAT3 activation was detected by Western blot.

(**c**) Effects of IL-6 and NO on human MDSC-induced breast cancer STAT3 phosphorylation. Human breast cancer MDA-MB-231 cells were cultured with MDSCs in transwell system in the presence of anti-IL-6 mAb and iNOS inhibitor for 6 hours. STAT3 phosphorylation was detected with Western blot.

(**d**) Effects of IL-6 and NO on breast cancer STAT3 phosphorylation. MCF-7 cells were treated with IL-6 and GSNO for different time periods. STAT3 phosphorylation was detected with Western blot. One of 3 experiments is shown.

(**e–g**) Effects of MDSCs on MCF-7 breast tumor growth in NSG mice. MCF7 cells were co-cultured with MDSCs in the presence of anti-IL-6 mAb and iNOS inhibitor, or isotype antibody for one hour, and inoculated subcutaneously into NSG mice supplied with E2 (estradiol-17β pellet). (e) Tumor growth was monitored. N = 5/group, *, $P < 0.05$ (Mann–Whitney U test); (f, g) ALDH1 cells in PAN-Keratin^{+} tumor cells were evaluated by immunofluorescence staining of paraffin-embedded tissues (f) Results are expressed as the mean relative values ± SEM (Mann–Whitney U test, $P < 0.05$; (g) One of 5 representative tissues is shown.

(**h**) Scheme of MDSC and CSC cross-talk. MDSCs activate STAT3 and NOTCH via IL-6 and NO, respectively. NOTCH activation facilitates and sustains persistent STAT3 activation via IL-6, and the cross-talk between IL-6/STAT3 and NO/NOTCH promote breast cancer stemness.